



THEORETICAL AND EXPERIMENTAL ANALYSIS OF A THERMOSYPHON USED IN COMPACT SOLAR COLLECTOR

Paulo Henrique Dias dos Santos
Monique Goto Holetz
Gabriel Nagib Zina
Larissa Krambeck
Thiago Miranda dos Santos
Celso Gonçalves de Quadros
Thiago Antonini Alves

Federal University of Technology - Paraná, Department of Mechanical Engineering, 84016-210, Ponta Grossa, PR, Brazil
psantos@utfpr.edu.br

Abstract. *The current paper presents a theoretical and experimental analysis of a copper thermosyphon which will be used in a compact solar collector. Its performance is influenced by the diameter, evaporator length, condenser length, work fluid and operating limits as boiling limit, viscous limit, limit drag and sonic limit. First, a mathematical model regarding the operation limits is presented. Next, the thermosyphon is tested for different heat loads varying from 40 up to 80 W in order to evaluate its performance regarding its operational limits. The theoretical and experimental results are compared in order to validate the mathematical model. After this validation, the mathematical model is used as an useful tool for design of thermosyphons for compact solar collectors.*

Keywords: *Copper Thermosyphons, Water, Compact Solar Collector*

1. Introduction

The heat pipes are highly efficient devices to thermal control because they can transfer large amounts of heat. They are largely used in different engineering applications, since aerospace application until thermal control microelectronics (Groll and Rosler, 1992a). The thermosyphons, also named by heat pipes assisted by gravity, are the simplest types of heat pipe and they have many applications in industrial heat recovery. Therefore, these devices are a viable alternative to solar collectors, due its relative simplicity of construction and the pumping of the working fluid done by gravity due the inclination of surface of the collector.

A new configuration for a compact solar collector assisted by thermosyphons for domestic water heating is here announced. Previous works presented application studies of heat pipes and thermosyphons in solar collector for domestic water heating using different configuration here announced. Oliveti and Arcuri (1996); Ismail and Abogderah (1992, 1998); Hussein *et al.* (1999b,a) presented results obtained with heat pipes applied in flat solar collectors where the heat pipes and thermosyphons condenser were immersed in a reservoir contained water in different cooling temperatures.

Oliveti and Arcuri (1996); Hussein *et al.* (1999b,a) used thrmosyphons with water as work fluid, while Ismail and Abogderah (1992, 1998) used heat pipes with an internal capillary structure in the evaporator region and methane as work fluid. Chun *et al.* (1999) presented a configuration where five thermosyphons are coupled in the collector and its condenser is cooled by a thermal bath with control temperatures. The collector was assisted by heat pipes and thermosyphons. Different work fluids (water, methane, acetone and ethanol) and different temperatures were tested for thermal bath in the condenser.

Abreu and Colle (2004) showed a different form from configurations previously mentioned because its condenser geometry. While others authors used straight pipes, his condensers were curved so the thermosyphons and thermal reservoir had a better fit. This solution allows a compact assembly and assured a better performance of the thermosyphons in case of low latitude, where the collector has a low slope. They developed an experimental apparatus to investigate basic design parameters in the thermosyphons' performance. This experiment helped to determine great dimensions on prototypes of solar collector assisted by thermosyphons to domestic water heating. They made tests with different length, slope and fill ratio for heat flux ranging from 400 to 1200 W/m².

This work presents theoretical and experimental analysis of a copper thermosyphon which will be used in a compact solar collector. For this analysis, a mathematical model regarding the operation limits and experimental results of the tested thermosyphon for different heat loads varying from 40 up to 80 W are presented.

2. Problem Description

The thermosyphon solar compact collector is showed in Fig. 1. This collector consists of five thermosyphons made of copper and using water as working fluid. The collector box is made of stainless steel and its underside is made of glass

through which the sunlight enters into it. In this region are allocated the evaporators of the thermosyphons. The condenser of thermosyphons are allocated on the top of the box, where a water flow passes outside surfaces of the tubes.

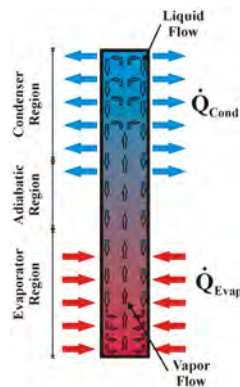


Figure 1. Sketch of the operating principle of thermosyphon.

The thermosyphon is composed of three parts: evaporator section, adiabatic section and the condenser section, as seen in Fig. 2. They operate as follows: the heat absorbed at the bottom the solar collector is transferred to the thermosyphon, vaporizing the fluid contained inside this region. The steam generated moves due to the pressure difference to cooler regions of the pipe condenser, where heat is rejected transported to the flow of water passing outside the tubes of the thermosyphon.

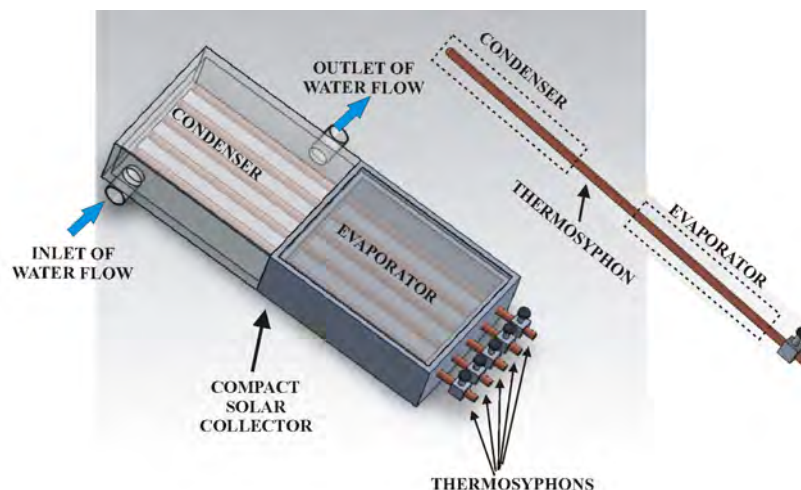


Figure 2. Sketch of the compact solar collector with two-phase closed thermosyphons.

In the heat rejection process, the steam condenses, and the condensate is transported back to the evaporator closing the cycle. The adiabatic region, which may have variable dimensions (being absent in some cases) is located between the evaporator and the condenser being isolated from the external environment. The return of the working fluid from the condenser to the evaporator is given by gravity. For this reason, the condenser must be located above the evaporator.

3. Mathematical Model

Here is presented the modeling of a thermosyphon that will be applied in a compact solar collector assisted by thermosyphons. The mathematical model is based on operating limits of thermosyphons (boiling limit, viscous limit, limit drag and sonic limit). Before started the study of limits, some analysis should be made to get the calculations easier. Deemed to be resistances in the walls of the thermosyphon, according to Fig. 3:

Where R_1 and R_9 are thermal resistances in the external surfaces of thermosyphon and can be calculated by:

$$R_1 = \frac{1}{h_{evap,out} A_{evap}} \quad (1)$$

$$R_9 = \frac{1}{h_{cond,out} A_{cond}} \quad (2)$$

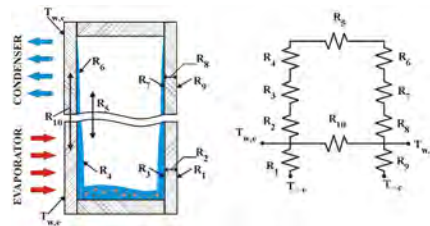


Figure 3. Thermosyphon resistances diagram.

The heat conduction resistance in the walls of the evaporator and condenser, respectively, are calculated by:

$$R_2 = \frac{\ln\left(\frac{d_{evap,out}}{d_{evap,in}}\right)}{2\pi l_{evap} k_w} \quad (3)$$

$$R_8 = \frac{\ln\left(\frac{d_{cond,out}}{d_{cond,in}}\right)}{2\pi l_{cond} k_w} \quad (4)$$

According to Groll and Rosler (1992b), the internal thermal resistances R_4 and R_6 related to changes in phase of the working fluid in the evaporator and condenser, respectively, are really small so they can be despised. Thus, the total thermal resistivity is given by (K/W):

$$R = R_1 + R_2 + R_8 + R_9 \quad (5)$$

It is assumed as first simplification to heat transfer rate:

$$\dot{Q} = \frac{\Delta T}{R} \quad (6)$$

$$q'' = \frac{4\dot{Q}}{\pi d_{evap,in}^2} \quad (7)$$

where ΔT is calculated as:

$$\Delta T = (T_{w,evap} - T_{w,cond}) \quad (8)$$

Due to thickness of the liquid film on the condenser is small, R_7 is neglected. Thus, the internal temperature of the working fluid in the vapor phase (saturation temperature) can be calculated by:

$$T_v = T_{w,evap} + (R_7 + R_8 + R_9)\dot{Q} \quad (9)$$

The fluid dynamic properties for the use of mathematical model are determined from the saturation temperature of the working fluid known. These properties are vapor pressure (p_v), liquid density (ρ_l), vapor density (ρ_v), latent heat of vaporization (h_{lv}), dynamic viscosity of liquid (μ_l), dynamic viscosity of vapor (μ_v), surface tension (σ).

After that is necessary understand what the operating limits are so its calculations may be performed.

3.1 Determination of the operating limits of thermosyphons

The operating limits of thermosyphons are: viscous limit, sonic limit, boiling limit and limit drag. Groll and Rosler (1992b) present a methodology to calculate these limits with equations lightly different from the ones assumed to heat pipes, these equations are going to be presented in this section. For the case of thermosyphons, the capillary limit, which is the most important limit for the heat pipes, isn't applied because thermosyphons don't have porous wick.

3.1.1 Viscous Limit

This type of limit is most common in cases of thermosyphons applied in low temperatures which can present a high length of condenser or thermosyphons. These factors make the difference of pressure in its internal be low, making a worst condition the passage of vapor from the evaporator to the condenser limiting the heat transportation.

The inertial forces become too low or negligible and the viscous forces become too high, been much higher than the difference of pressure in the interior of the thermosyphon, generating a condition of null vapor flux. To determinate the

viscous limit, two initial consideration are necessary: the working fluid is considered as a perfect gas and its flow is fully developed laminar. The viscous limit is calculated by:

$$q''_{max,viscous} = r_v^2 h_{lv} \frac{\rho_v p_v}{16 \mu_v l_{evap}} \quad (10)$$

3.1.2 Sonic Limit

This limit can appears when the heat rate removed from the condenser becomes too high, which makes the temperature of this region gets lower and increase the speed of the vapor in the end of the evaporator, that may achieves the sound speed.

Normally, as the heat transfer rate is increased, the flow of steam also increases. As more heat is removed from the condenser, the movement of the vapor in its inside will get faster to ends the loop. Increasing the speed vapor until it gets a sonic level, the pressure in the condenser will get lower. Recovering the normal pressure, a front shock can be formed, that will be compromise the operation of thermosyphon. To calculate the sonic limit, the working fluid can be considered as a perfect gas, the inertial forces are dominated and dragging effects are ignored. To know if the sonic limit is achieved, uses the following expression:

$$q''_{max,sonic} = 0,474 h_{lv} (\rho_v p_v)^{1/2} \quad (11)$$

3.1.3 Boiling Limit

This kind of limit occurs when the thermosyphon is too much filled with working fluid or when too much heat is provided to the pipe. With large amount of heat supplied to the evaporator, the working fluid is heated until it changes its phase to vapor, however critical heat flux causes bubbles form within the tube when this limit is reached. These bubbles coalesce, making a worst condition the passage of vapor to the condenser and the liquid to the evaporator, which may cause premature drying.

The bubbles get together joining the inner wall of the tube may cause melting of the material depending on its melting point. This occurs because the thermal conductivity of the bubbles is too low and the temperature of the wall increases continuously. In cases where the length of the thermosyphon be large relative to its diameter, this type of limit will almost never achieved, however the drag limit can appears for reason that will be explained after.

To check if the boiling limit is achieved, may determine the maximum load of radial heat being supplied. First, the value of K_L (parameter latent heat) must be calculated by the equation:

$$K_L = h_{lv} [\rho_v^2 (\rho_l - \rho_v) g \sigma]^{1/4} \quad (12)$$

Then, the maximum radial heat flow is defined by:

$$q''_{max,rad} = 0,12 K_L \quad (13)$$

$$\dot{Q}_{max,boiling} = q''_{max,rad} A_{evap} \quad (14)$$

where A_{evap} is the area of the evaporator given by:

$$A_{evap} = \pi d_{evap} l_{evap} \quad (15)$$

3.1.4 Drag Limit

As the vapor is condensed and goes back to the evaporator, a liquid film is formed in the inner wall of the tube. When the heat provided to evaporator is increased, the evaporation rate of the working fluid also increases, causing a phenomenon of instability inside the thermosyphon. The higher the speed that the vapor directs itself to the condenser, the shear forces of the waves may be increased. If these shear forces become too much bigger than the surface tension of the liquid, particles of the liquid film will be drag with the vapor to condenser, decreasing the efficiency of thermosyphon.

This type of limit is commonly founded in thermosyphons where the length / diameter ratio is large. The drag limit is calculated by:

$$q''_{max,drag} = 0,64 \left(\frac{\rho_l}{\rho_v} \right) \left(\frac{d_i}{4l_{cond}} \right) h_{lv} \sigma g \rho_v (\rho_l - \rho_v) \quad (16)$$

3.2 Heat Transfer Model for the Thermosyphon

This mathematic model is based on heat transfer correlation and in experimental measures obtained in the test rigs already exists in the LabCTEE (UTFPR-PG). Here, will be presented a methodology to analyze of only one thermosyphon. It's Intend, along of this project, extend and improve this model based on heat transfer to the project of compact collector solar assist by thermosyphon. For this, will be include heat transfer terms by radiation and convection taking in consideration the working fluid phase change of the thermosyphon.

In the Fig. 4 is presented a thermosyphon schematic drawing used to modeling with its respective temperature measure points T_{evap1} , T_{evap2} and T_{evap3} located in the evaporator surface, T_{ad1} and T_{ad2} located in the surface of the adiabatic section, T_{cond} located in the condenser surface and the temperatures measures points T_{in} and T_{out} located in the water flow used in the system condensation by water of the thermosyphon condenser.

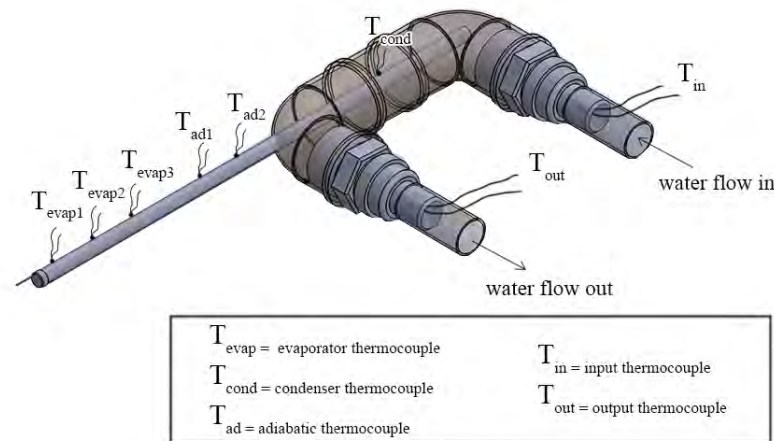


Figure 4. Positions of the thermal sensors along the thermosyphon.

When a energy balance is done in the thermosyphon, can say that the heat transfer ratio that is applied to the evaporator (\dot{Q}_{evap}) is equal the heat transfer ratio to the environment through the thermal insulation (\dot{Q}_{ins}) and to the condensation system by water of the condenser (\dot{Q}_{cond}), that is,

$$\dot{Q}_{evap} = \dot{Q}_{ins} + \dot{Q}_{cond}. \quad (17)$$

When the inlet (T_{in}) and outlet (T_{out}) temperatures and the mass flow (\dot{m}_{water}) of the water flow of the condensation system are measured, can determine the lost heat transfer ratio in the condenser region of the thermosyphon, considering the water specific heat constant, of the following way:

$$\dot{Q}_{cond} = \dot{m}_{water} c_{p,water} (T_{out} - T_{in}). \quad (18)$$

According to Incropera and DeWitt (2003), the heat transfer rate through the thermal insulation (\dot{Q}_{ins}) across of a cylinder can be estimated with the follow expression:

$$\dot{Q}_{ins} = \frac{(T_w - T_{amb})}{\left[\left(\frac{\ln(d_{ins}/d_{evap,out})}{2\pi k_{ins}} \right) + \left(\frac{1}{h_{air} 2\pi d_{ins} L_{ins}} \right) \right]} \quad (19)$$

The heat transfer coefficient by natural convection of the air (h_{air}) is estimated of this way:

$$h_{air} = \frac{Nu_{air} k_{air}}{d_{ins}} \quad (20)$$

The Nusselt number of the air (Nu_{air}) can be determined using the correlation proposed by Churchill and Chu (Incropera and DeWitt, 2003):

$$Nu_{air} = \left\{ 0.60 + \frac{0.387 Ra^{1/6}}{\left[1 + (0.559 / Pr_{air})^{9/16} \right]^{8/27}} \right\}^2 ; \quad Ra \leq 10^{12} \quad (21)$$

P.H.D. Santos, M.G. Holetz, G.N. Zina, L. Krambeck, T.M. Santos, C.G. Quadros, T.A. Alves
Theoretical and Experimental Analysis of A Thermosyphon Used in Compact Solar Collector

According to Incropera and DeWitt (2003), the Rayleigh number can be estimated by the below correlation:

$$Ra = \frac{g\beta_{air}(T_w - T_{amb})L_{ins}^3}{\nu_{air}\alpha_{air}}, \quad (22)$$

All the thermodynamics properties were determined in function of the film temperature (T_f) which is related as follow:

$$T_f = \frac{(T_w + T_{amb})}{2} \quad (23)$$

4. Description of the Experimental Device and the Test Rig

The methodology for manufacturing, tests and analyses of the thermosyphon here developed is based on Reay and Kew (2006). A thermosyphon was made of a copper tube with outer diameter of 12.7 mm (1/2 in). The thermosyphon has a evaporator length of 160 mm, a adiabatic length of 90 mm and a condenser length of 250 mm. The Fig. 5 shows the thermosyphon and the Table 1 presents all the features about the thermosyphon and the working fluid.

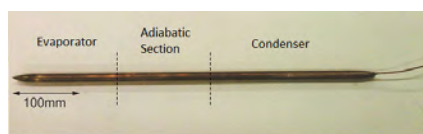


Figure 5. General view of the thermosyphon.

Table 1. Structural characteristics of the thermosyphon.

| Characteristic | Thermosyphon |
|-------------------------|--------------|
| Inner diameter | 10.7 mm |
| Outer diameter | 12.7 mm |
| Evaporator length | 160.0 mm |
| Adiabatic region length | 90.0 mm |
| Condenser length | 250.0 mm |
| Working fluid | Water |

Before the liquid filling of the thermosyphon with dionized water, it is necessary to make vacuum inside the tube. During the vacuum process the pressure inside reached was 90 mbar (9 kPa) and the saturation temperature related to this pressure was 43.74 °C. At the moment of the filling it is necessary to be very careful so that the existing vacuum in the tube is not lost. If it happens, the whole vacuum process should be repeated.

The amount of working fluid inserted inside the thermosyphon is very important for the two-phase system, because the heat transfer depends on that amount of fluid into the evaporator region. Therefore, the thermosyphon was filled according to the literature (Abreu and Colle, 2004) with 35 ml of water which correspond to 70% the thermosyphon volume.

Fig. 6 presents the thermosyphon with the cooling system at the condenser section and the heating system of the evaporator. The thermosyphon was heated using by a power supply which applied a potential difference around the evaporator using a copper wire as an electrical resistor. The heat sink of the condenser used water as working fluid and was cooled by a thermostat.

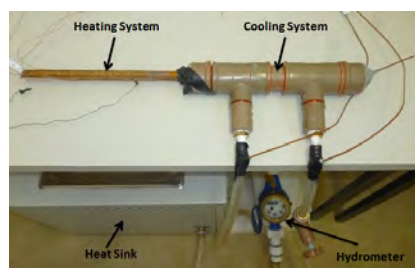


Figure 6. View of the thermosyphon, showing the heating and the cooling systems.

Fig. 7 shows the experimental setup used to test the thermosyphon. There is a power source that applies heat and there is a thermostatic heat sink which provides cooling water in the condenser region.

Fig. 8 presents the detailed view of the thermosyphon installed on the test rig. The thermosyphon was tested only at a slope of 90°.

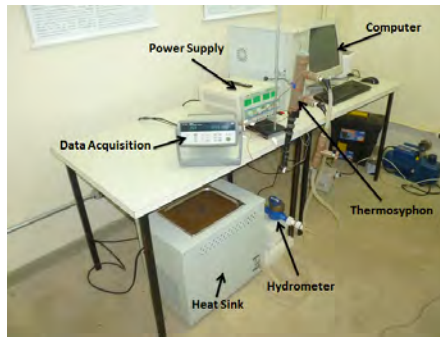


Figure 7. View of the test rig.

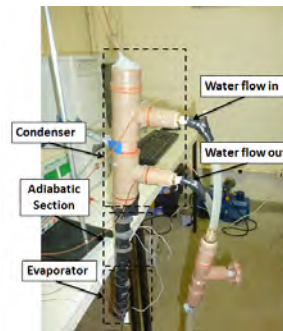


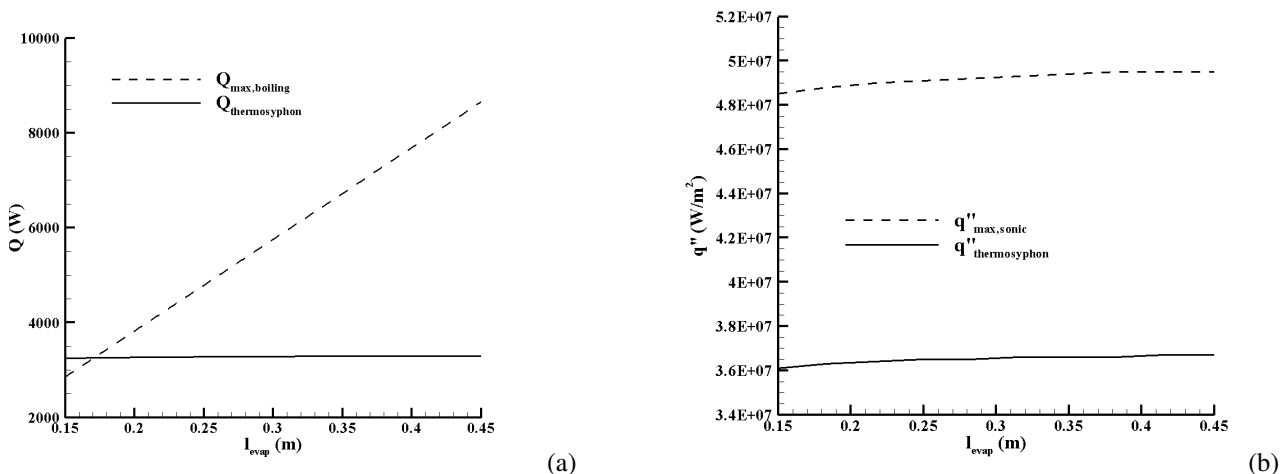
Figure 8. Detailed view of the thermosyphon installed on the test rig.

5. Results and Discussion

5.1 Theoretical Results

The working fluid here utilized was water. The thermal and hydrodynamic properties could be determined as a function of vapor temperature which was calculated by Eq. 7 ($T_v = 56,6 \text{ }^\circ\text{C}$). The data used to make the calculation were: $T_{out,e} = 90 \text{ }^\circ\text{C}$ and $T_{out,c} = 27 \text{ }^\circ\text{C}$, a tube made of copper, thickness 1 mm, coefficient of heat transfer in outside of evaporator $31 \text{ W/m}^2\text{-K}$, coefficient of heat transfer in outside of condenser $37 \text{ W/m}^2\text{-K}$. Some dimension parameters were varied to determine what influence they cause in operating limits of thermosyphons. The lengths of the evaporator and condenser were varied from 15 to 45 cm. The outer diameter of the thermosyphon was also modified from 0.5 in (12.7 mm) and 2 in (50.8 mm).

Figs. 9(a) and 9(b) show the boiling limit and sonic limit, respectively, as a function of the length variation of evaporator. Noticed that when the length is smaller than 17.5 cm, the boiling limit is achieved, thus the thermosyphon will not be able to work. Observe also that the sonic limit is not achieved. The drag limit and the viscous limit were too much higher than the heat load of the thermosyphon, from 1.028×10^{10} up to $1.031 \times 10^{10} \text{ W/m}^2$ (drag limit) and from 1.7×10^9 up to $4.9 \times 10^9 \text{ W/m}^2$ (viscous limit).

Figure 9. (a) Boiling limit and (b) Sonic limit as a function of the l_{evap} variation.

Figs. 10(a) and 10(b) show the boiling limit and sonic limit, respectively, as a function of the length variation of condenser. Noticed that the boiling limit and sonic limit are not achieved. The drag limit and the viscous limit were too much higher than the heat load of the thermosyphon, from 5.7×10^9 up to 1.7×10^{10} W/m² (drag limit) and from 2.94×10^9 up to 3.08×10^9 W/m² (viscous limit).

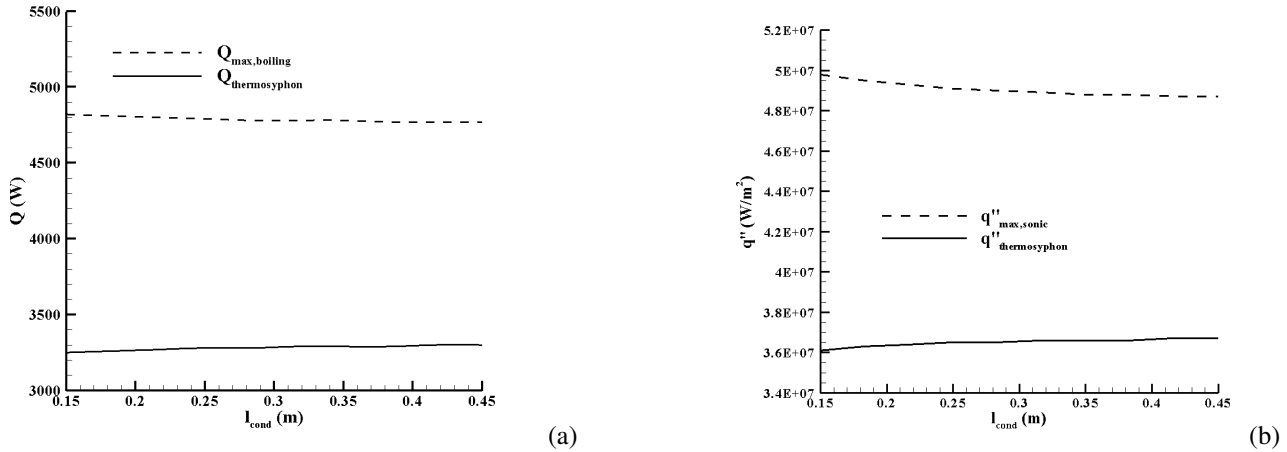


Figure 10. (a) Boiling limit and (b) Sonic limit as a function of the l_{cond} variation.

Figs. 11(a) and 11(b) show the boiling limit and sonic limit, respectively, as a function of variation of the outer diameter of thermosyphon. Boiling limit and sonic limit are not achieved. The drag limit and the viscous limit were too much higher than the heat load of the thermosyphon, from 1.03×10^{10} up to 4.70×10^{10} W/m² (drag limit) and from 3.0×10^9 up to 6.2×10^{10} W/m² (viscous limit).

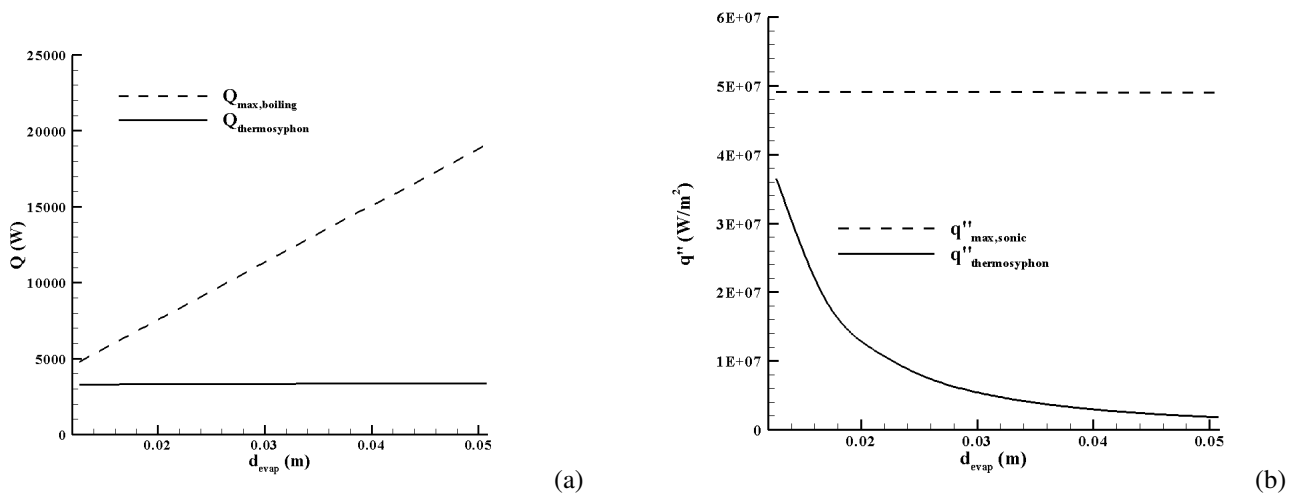


Figure 11. (a) Boiling limit and (b) Sonic limit as a function of the d_{evap} variation.

5.2 Experimental Results

The thermosyphon was tested for an increasing heat loads from 40 to 80 W (Fig. 12). This figure shows the temperatures along the thermosyphon: evaporator ($T_{Evaporator,1}$, $T_{Evaporator,2}$ and $T_{Evaporator,3}$), adiabatic region ($T_{Adiabatic,1}$ and $T_{Adiabatic,2}$) and condenser ($T_{Condenser,1}$).

As expected, when the heat load of 40 W is applied the temperatures of evaporator ($T_{Evaporator,1}$, $T_{Evaporator,2}$ and $T_{Evaporator,3}$) increase sharply as well as the temperatures of adiabatic region ($T_{Adiabatic,1}$ and $T_{Adiabatic,2}$). These temperatures continue increasing until time of 200 s, when they reach a specific peak. After this peak, the temperatures start to decrease sharply. At time of approximately 200 s, the temperature of condenser ($T_{Condenser,1}$) starts to increase and this coincides with the decrease of evaporator and adiabatic region temperatures. This is due to the start-up of the thermosyphon. Heat is supplied to the evaporator until the liquid becomes vapor and this vapor flows to the condenser. When the liquid-vapor phase change happens heat is removed, the temperatures of the evaporator and adiabatic region are decreased. The increasing of the condenser temperature is due to the generated vapor goes inside the condenser and as a consequence the condenser temperature starts to increase.

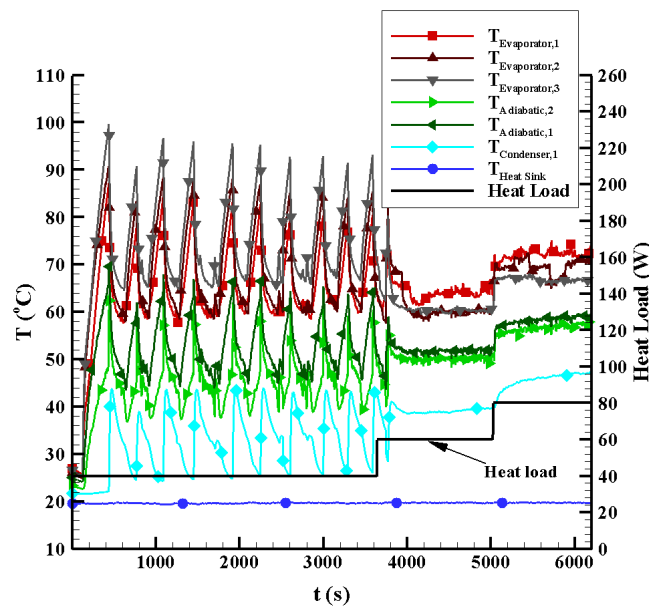


Figure 12. Temperatures of the thermosyphon for heat loads increasing.

It can be noticed a oscillatory thermal behavior of the thermosyphon. After the start-up, the temperatures of evaporator and adiabatic region decrease until time approximately 800 s. Next, these temperatures start to increase and the condenser temperature decreases. So, according to this result, as the temperatures of evaporator is not being controlled, the liquid-vapor phase change is not occurring and no more vapor goes inside the condenser. As a result, the condenser temperature decreases. To some extent, this is caused because there is no sufficient return of liquid from condenser to the evaporator. This oscillatory thermal behavior continues until the heat load increases for 60 W. Now, the liquid return is enough and the temperatures reach a steady state condition. The heat load is increased up to 80 W and the thermosyphon worked successfully. Under steady state and heat load of 80 W, the maximum temperature reached was approximately 74 °C.

Fig. 13 presents the heat transfer analysis for the thermosyphon under studied. The heat transfer rates (\dot{Q}_{evap} , \dot{Q}_{ins} and \dot{Q}_{cond}) were estimated using the Eqs. 17 to 23 presented in the section 3.2 and the experimental results as presented in Fig. 12. The oscillatory thermal behavior was neglected and the \dot{Q}_{evap} was evaluated for 60 and 80 W. It can be noticed nevertheless that the \dot{Q}_{cond} presented a oscillatory thermal behavior with average heat transfer rates of about 40 W ($\dot{Q}_{evap} = 60W$) and 55 W ($\dot{Q}_{evap} = 80W$). The \dot{Q}_{ins} varied from 3.2 up to 6.4 W. Thus, It can be noticed that 16.8 W (about 28% of the 60 W applied to the evaporator) and 18.6 W (about 23% of the 80 W applied to the evaporator) are not taking into account in this model, showing that it could be improved in future works.

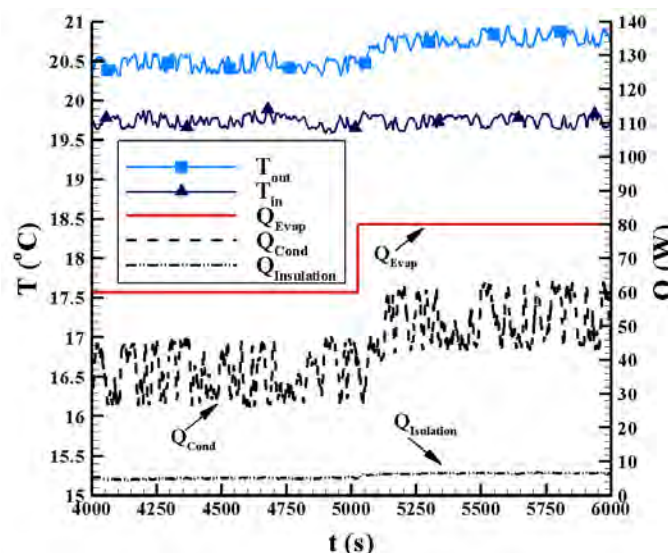


Figure 13. Heat transfer analysis of the thermosyphon for heat loads increasing.

P.H.D. Santos, M.G. Holetz, G.N. Zina, L. Krambeck, T.M. Santos, C.G. Quadros, T.A. Alves
Theoretical and Experimental Analysis of A Thermosyphon Used in Compact Solar Collector

6. Conclusion

This paper presents a methodology based on experimental tests and on a mathematical modeling for developing thermosyphons that could be applied in thermosyphon solar compact collectors. The methodology here presented is focused on only one thermosyphon, but it can be extended to a set of thermosyphons. The mathematical modeling was based on operating limits of thermosyphons. The geometric parameters of thermosyphon analyzed were: outer diameter of thermosyphon, lengths of the evaporator and condenser. With length of evaporator smaller than 17.5 cm, the thermosyphon can be failed due to the boiling limit achievement. The sonic limit, drag limit and viscous limit are not critical in the developing this type of thermosyphon.

Based on the theoretical results obtained with the mathematical model, a thermosyphon was manufactured of copper and using water as working fluid and with evaporator length of 16 mm. Experimental tests were run out for increasing heat load (from 40 up to 80 W) at a slope of 90° with the condenser above the evaporator. Therefore, it could be concluded that this model could predict the theoretical limit for success operation of the thermosyphon, showing that the mathematical model should be used in the design of kind of thermosyphon.

According to the heat transfer analysis of the thermosyphon, 16.8 W (about 28% of the 60 W applied to the evaporator) and 18.6 W (about 23% of the 80 W applied to the evaporator) are not taking into account in the heat transfer model. Therefore, this model should be improved in future works.

7. ACKNOWLEDGEMENTS

The authors thank the National Council for Scientific and Technological Development (CNPq), a foundation linked to the Ministry of Science and Technology and Innovation (MCTI), as well as the Federal University of Technology - Paraná.

8. REFERENCES

- Abreu, S.L. and Colle, S., 2004. "An experimental study of two-phase closed thermosyphons for compact solar domestic hot-water systems". *Solar Energy*, Vol. 76, pp. 141–145.
- Chun, W., Kang, Y., Kwak, H. and Lee, Y., 1999. "An experimental study of the utilization of heat pipes for solar water heaters". *Applied Thermal Engineering*, Vol. 19, pp. 807–817.
- Groll, M. and Rosler, S., 1992a. "Operation principles and performance of heat pipes and closed two-phase thermosyphons". *Journal of Non-Equilibrium Thermodynamics*, Vol. 17, pp. 91–151.
- Groll, M. and Rosler, S., 1992b. "Operations principles and performance of heat pipes and closed two-phase thermosyphons: and overview". *Journal of Non-Equilibrium Thermodynamics*, Vol. 17, pp. 91–151.
- Hussein, H.M.S., Mohamad, M.A. and El-Asfour, A.S., 1999a. "Optimization of a wickless heat pipe flat plate collector". *Energy Conversion and Management*, Vol. 40, pp. 1949–1961.
- Hussein, H.M.S., Mohamad, M.A. and El-Asfour, A.S., 1999b. "Transient investigation of a thermosyphon flat-plate solar collector". *Applied Thermal Engineering*, Vol. 19, pp. 789–800.
- Incropera, F.P. and DeWitt, D.P., 2003. *Fundamentals of Heat and Mass Transfer*. John Wiley & Sons, Inc.
- Ismail, K.A.R. and Abogderah, M.M., 1992. "Residential solar collector with heat pipes". In *8th International Heat Pipe Conference, Beijing, China*.
- Ismail, K.A.R. and Abogderah, M.M., 1998. "Performance of a heat pipe solar collector". *Journal of Solar Energy Engineering*, Vol. 120, pp. 51–59.
- Olivetti, G. and Arcuri, N., 1996. "Solar radiation utilisability method in heat pipe panels". *Solar Energy*, Vol. 57, pp. 345–360.
- Reay, D. and Kew, P., 2006. *Heat Pipes - Theory, Design and Applications*. Elsevier Science and Technology.

9. RESPONSIBILITY NOTICE

The authors are the only responsible for the printed material included in this paper.